Supramolecular Chemistry
Publication details, including instructions for authors and subscription information:
http://www.informaworld.com/smpp/title~content=t713649759

Recognition of sugars and related compounds by "reading-out"-type interfaces

Tony D. James[a]; K. Samankumara Sandanayake[a]; Seiji Shinkai[a]
[a] Shinkai Chemirecognics Project, Kurume, Fukuoka, Japan

To cite this Article James, Tony D. , Sandanayake, K. Samankumara and Shinkai, Seiji(1995) 'Recognition of sugars and related compounds by "reading-out"-type interfaces', Supramolecular Chemistry, 6: 1, 141 — 157
To link to this Article: DOI: 10.1080/10610279508032530
URL: http://dx.doi.org/10.1080/10610279508032530

SUPRAMOLECULAR CHEMISTRY, Vol. 6, pp. 141–157
Reprints available directly from the publisher
Photocopying permitted by license only

Recognition of sugars and related compounds by "reading-out"-type interfaces

TONY D. JAMES, K. R. A. SAMANKUMARA SANDANAYAKE and SEIJI SHINKAI*

Shinkai Chemirecognics Project, ERATO, Aikawa 2432-3, Kurume, Fukuoka 830, Japan

(Received August 5, 1994)

INTRODUCTION

The vast number and diversity of saccharides in nature are the ultimate challenge for the 'Host-Guest' Chemist. Two areas in particular have stimulated our interest:

i) Saccharide recognition in water:
The recognition of D-glucose is of particular interest, since the breakdown of glucose transport has been correlated with certain diseases: renal glycosuria,[1,2] cystic fibrosis,[3] diabetes[4,5] and also human cancer.[6] The study of glucose and other monosaccharide gradients *in vivo* is therefore of seminal importance.

ii) Colour control:
How do the plethora of colours in nature arise? In most flowers the subtle change in colour and tone is controlled by intermolecular and/or intramolecular interactions between saccharides covalently-bound to the anthocyanin dye.[7,8] Our aim in the present research is to reproduce such a saccharide-induced colour change in a totally artificial system.

BORONIC ACIDS; THE BASICS

Our group[9–24] and others[25–30] have started to exploit the interactions of boronic acids with saccharides[31]. Such interactions we believe can be exploited in the development of receptor sites for saccharide detectors. We have found that certain facets of the boronic acid character must be borne in mind when designing new receptors for saccharides:

(i) sp^2 Boron is readily converted to sp^3 boron in the presence of Lewis bases.
(ii) If the Lewis base interaction is stronger than that of OH (for example OR or nitrogen) the acidity of the boronic acid increases.[32]

DYE MOLECULES

As mentioned in the introduction, the design of dye molecules is driven by two desires, one is the simply aesthetic desire to mimic the colours of flowers and the other is to use colour as a tool in the detection of *in vivo* concentrations of saccharides.

Two approaches employing azobenzene dyes have been employed:

i) Colour by deagregation:[20]
When boronic acid $RB(OH)_2$ forms complexes with sugars, they become more hydrophilic. If $RB(OH)_2$ is appropriately appended to chromophores which tend to aggregate in water, then the aggregation-deaggregation equilibrium should be controlled by the concentration, absolute configuration and complex stoichiometry of the added saccharides and the process 'read-out' as a colour change: that is, the boronic acid moiety acts as a 'sugar interface'.

The pK_a of the boronic acid **1** is 8.7 in the absence of saccharides and 5.6 in the presence of 0.10 M D-fructose. The largest difference in the absorption spectra will be observed at pH 6.9 by addition of saccharides. The concentration-dependence of **1** did not obey the Beer-Lambert law and gave a new peak at 385 nm at higher concentrations. The spectral shape changed when DMF was added to the aqueous solution (Figure 1). The results indicate that **1** aggregates in this medium. We thus added

*To whom correspondence should be addressed.

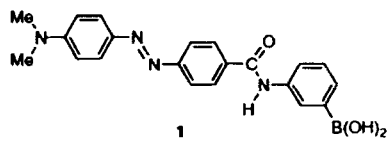

1

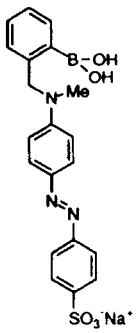

2

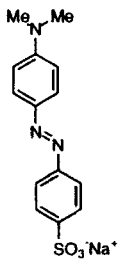

3

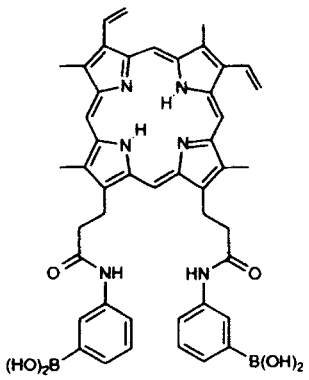

4

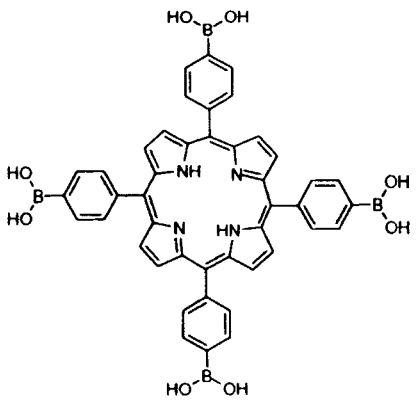

5

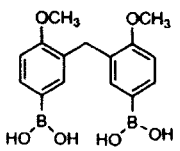

6

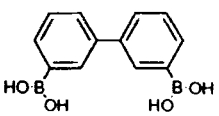

7

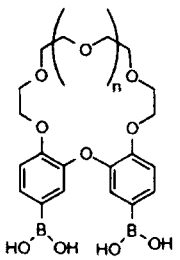

8a: n=0

8b: n=1

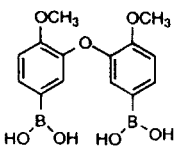

9

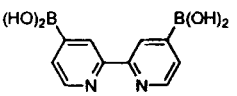

10

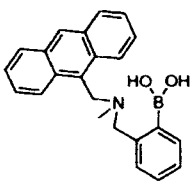

11

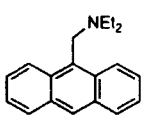

12

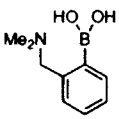

13

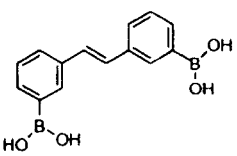

14

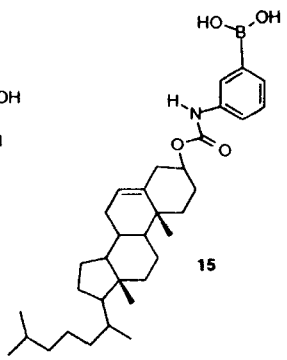

15

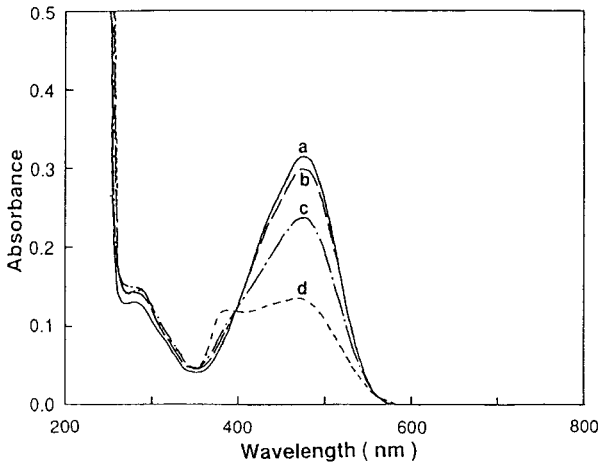

Figure 1 Absorption spectra of **1** (1.00×10^{-5} M) at 25°C and pH 6.9 (0.10 M phosphate): water:DMF (v/v) = 5:1 (a), 10:1 (b), 20:1 (c), and 300:1 (d).

several monosaccharides, expecting that complexation between **1** and monosaccharides induces deaggregation of **1**. Very interestingly, *the color of the solution changed from yellow to orange*: the corresponding absorption spectra are shown in Figure 2. The λ_{max} at 385 nm disappears as the λ_{max} at 472 nm increases with an isosbestic point at 391 nm. The absorption spectrum in the presence of D-fructose is very similar to that in the presence of the SDS (100 mM) micelle in which **1** is dispersed discretely.

Figure 3 shows plots of monosaccharide concentration vs. OD_{472}. The magnitude of the spectral change corresponds with the order of association constants for simple boronic acids: that is, D-fructose>D-arabinose>D-mannose>D-glucose.[9,25,32,33] This result, together with those described above, supports the view that the color

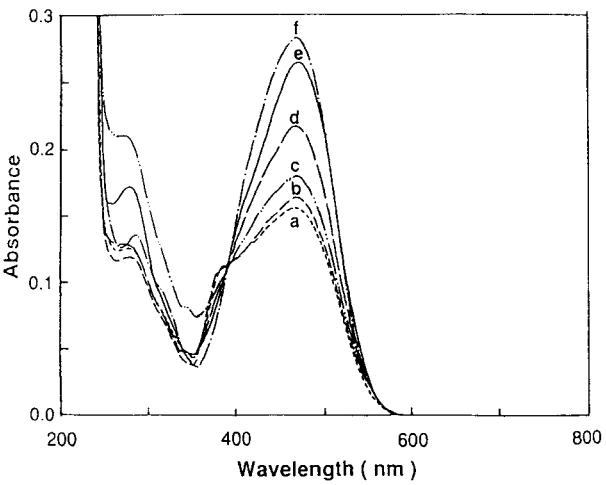

Figure 2 Absorption spectra of **1** (1.00×10^{-5} M) at 25°C and pH 6.9 (0.10 M phosphate): water:DMF = 300:1 v/v: no saccharide (a), [saccharide] = 0.10 M D-glucose (b), D-mannose (c), D-arabinose (d), D-fructose (e), and no saccharide in the presence of the SDS (100 nm) micelle (f).

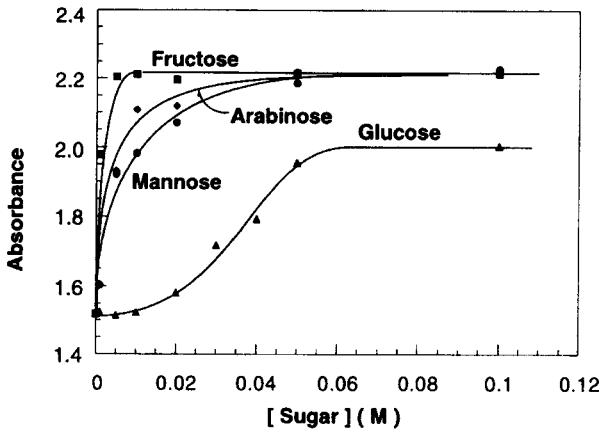

Figure 3 Plots of [saccharide] vs. OD_{472} at [**1**] = 1.00×10^{-3} M at 25 °C and pH 10.5 (0.10 M carbonate): water:DMF = 300:1 v/v.

change is related to deaggregation of monosaccharides induced by the saccharide-binding which makes **1** more hydrophilic.

ii) ICT (Internal Charge Transfer) molecular sensor:[19] This colour sensor for saccharides is based on the interaction found between boronic acid and a neighboring amine group. The amine interaction makes the boronic acid moiety more acidic hence lowering the working pH of the sensor molecule[18,30]. Rationally designed molecule **2** utilizes these effects. The anilinic electron donor moiety of the ICT chromophore is assembled as the neighbouring group participant to the boronic acid- saccharide interaction. It is well known that the pK_a of the boronic acid is increased by the saccharide interaction[25,30,32]. The electronic changes associated with this pK_a change could be directly transmitted to the neighbouring amine moiety creating a spectral change in the ICT chromophore. The complexation process can be read-out by the spectral change.

The absorption pH profile for the molecular sensor **2** in aqueous media with different saccharides is given in Figure 4 and 5. The step found at low pH range (pK_{a2} = 2.60) is due to the protonation of the anilinic moiety. The boronic acid amine interaction has shifted this equilibrium towards low pH compared to the parent chromophoric molecule **3** (pK_a = 3.7). The second step (pK_{a1} = 9.76) is believed to be due to the association equilibrium of the boronic acid with the amine moiety. The most important species involved and the equilibrium process are given in Scheme 1. The introduction of D(-)-fructose into the solution shifts the second equilibrium (pK_{a2}) by 0.28 pK_a units and more importantly the first equilibrium (pK_{a1}) by 3.31 pK_a units (Table 1 and Figure 4). D(+)-Glucose gave a relatively small shift and ethylene glycol, which is less preorganized (as a *cis* diol), gave almost no change. The saccharide titration at pH 7.6 gave a small absorption spectral change and a very low

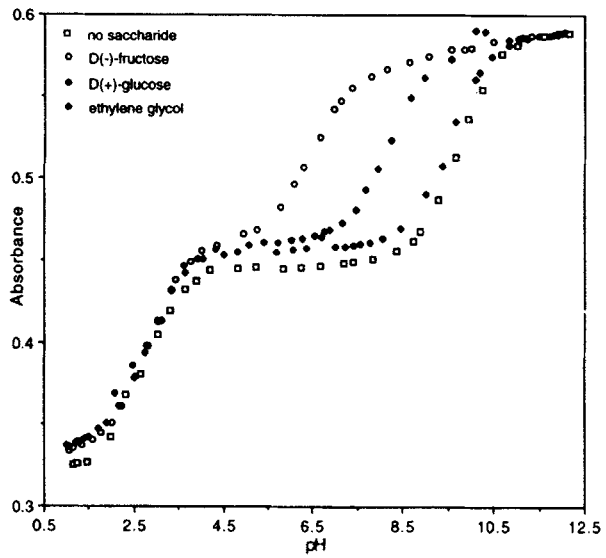

Figure 4 Absorption-pH profile of **2** with saccharides. 0.05 M saccharide and 0.05 M NaCl.

stability constant for glucose; ethylene glycol did not give any measurable spectral changes. D(-)-Fructose gave large spectral changes (log$K$ = 2.14) as expected from the pH titration curve. Saccharide binding to boronic acid is expected to be at the 1,2 diols in the case of glucose and 1,3 diols in the case of fructose creating five-membered and six-membered rings, respectively.[18]

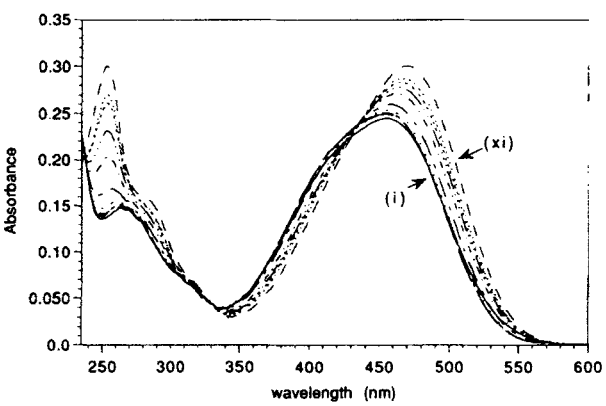

Figure 5 Absorption spectral changes of **2** at different pH with 0.05 M D(+)-glucose and 0.05 M NaCl: pH=4.34 (i), 5.39 (ii), 6.49 (iii), 6.98 (iv), 7.41 (v), 7.88 (vi), 8.39 (vii), 8.71 (viii), 9.07 (ix), 9.23 (x), 10.64 (xi).

Table 1 The influence of saccharides on the pK_as of **2** in aqueous media with 0.05 M NaCl

	pK_{a1}	ΔpK_{a1}	pK_{a2}	ΔpK_{a2}
D(-)-fructose	6.45	3.31	2.88	0.28
D(+)-glucose	8.29	1.47	2.78	0.18
ethylene glycol	9.54	0.22	2.75	0.15
no saccharide	9.76	—	2.60	—

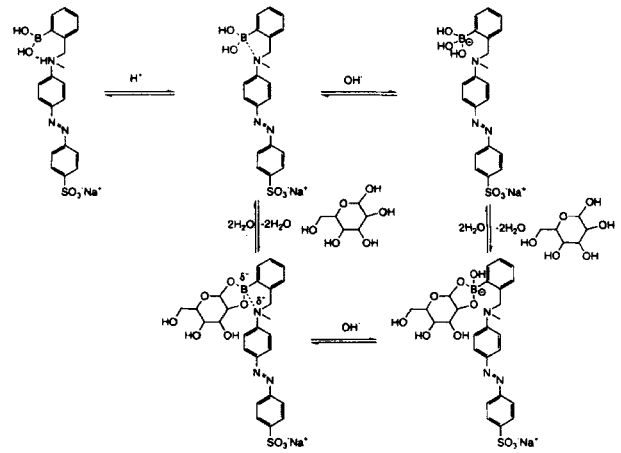

Scheme 1

PORPHYRINS

The aggregation behaviour of porphyrins with appended boronic acids are altered by added saccharide[21]

Figure 6 shows the absorption spectra of **4** in DMSO-water mixed solvents. The sharp peak (λ_{max} 405 nm) in DMSO, which is attributed to monomeric **4**, was gradually flattened with increasing water concentration. The broad peak (l_{max} 375 nm) is attributable to aggregated **4**. When sodium dodecylsulphate (SDS: 0.10 M) was added to the aqueous solution, the peak became sharp again, indicating that **4** is solubilized discretely in the SDS micelle. The results show that the absorption spectrum of **4** changes in response to a shift of the aggregation-deaggregation equilibrium. Hence, one can expect a similar spectral change if complexation of the appended boronic acids with saccharides induces deaggregation of **4** in water. In general, complexation of boronic acids with saccharides is expressed as in Scheme 2. We measured the absorption spectra of **4** at pH 6.9 – 11.0 in the absence and the presence of 0.10 M D-fructose. The largest spectral change was observed at pH 10.5. We thus employed this pH for the subsequent measurements. Since this pH is higher than pK_a of boronic acids (*ca.* 9),[25,30] the change induced by saccharide addition corresponds to the change from $RB^-(OH)_3$ to the saccharide bound boronate anion.

With increasing D-fructose concentration the absorbance gradually increased and the λ_{max} at 375 nm shifted to 380 nm (ϵ 8.9 × 10^4 $M^{-1}cm^{-1}$). According to Inamura and Uchida,[34] protoporphyrin dispersed in basic aqueous solution gives the Soret band at 380 nm (ϵ 9.5 × 10^4 $M^{-1}cm^{-1}$), which is ascribed to the dimer. The coincidence in λ_{max} and ϵ supports the view that the binding of D-fructose to the boronic acids changes aggregated **4** to dimeric **4**. In Figure 7, the absorbance at 380 nm was plotted against sugar concentrations. Among the four monosaccharides tested, D-fructose showed the largest spectral change. In contrast, the spectrum of protoporphyrin without boronic acids was scarcely changed by

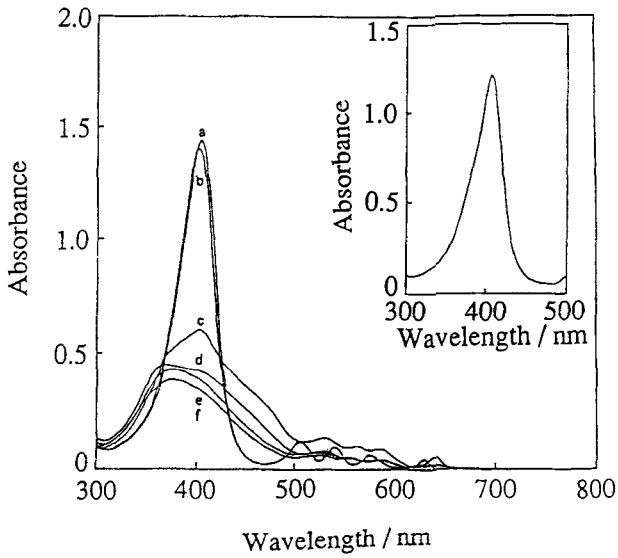

Figure 6 Absorption spectra of **4** (1.00×10^{-5} M) at 25°C in (a) DMSO, (b) DMSO:water = 2:1 v/v, (c) DMSO:water = 1:1 v/v, (d) DMSO:water = 1:2 v/v, (e) DMSO:water = 1:30 v/v and (f) DMSO:water = 1:300 v/v. The inserted spectrum is in DMSO: water = 1:30 v/v in the presence of 0.10 M SDS.

the addition of these monosaccharides. The results support the view that deaggregation of **4** is induced by complexation of monosaccharides with the boronic acid moieties which enhances the solubility of **4** in water.

We found that the sugar-binding process can be readout more sensitively by fluorescence. In the absence of monosaccharides, **4** was nonfluorescent because of aggregation (Figure 8). With increasing monosaccharide concentrations the fluorescence intensity at 632 nm increases conspicuously. Among four monosaccharides tested herein, D-fructose again showed the largest fluorescence increase (Figure 9). We have confirmed that even 0.5 mM of D-fructose can be detected by this method. In contrast, the fluorescence change in protoporphyrin without boronic acids was scarcely induced by the addition of these four monosaccharides.

What is the origin of saccharide-induced spectral changes? The association constants of monosaccharides

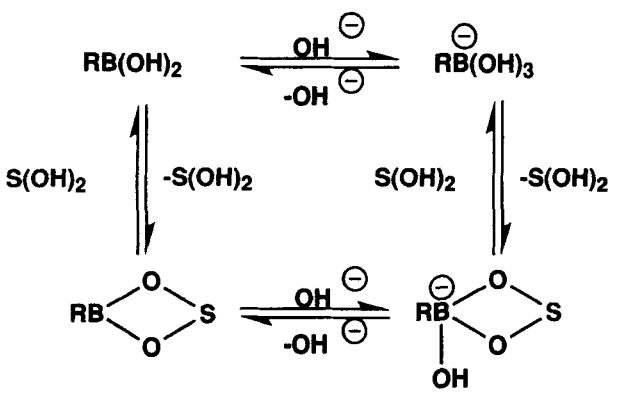

Scheme 2

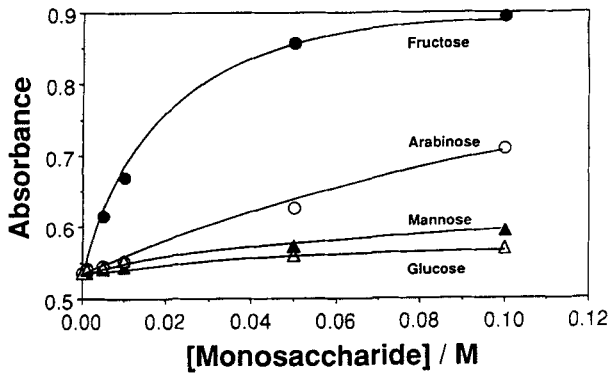

Figure 7 Absorbance increase at 380 nm plotted against monosaccharide concentrations.

for boronic acids have been determined.[9,25,32,33] The order of the association constants is exactly in line with the order of the spectral change: *i.e.*, D-fructose>D-arabinose>D-mannose ≥ D-glucose. This implies that complexation of the boronic acids with monosaccharides makes **4** more hydrophilic and the monosaccharide that shows the higher affinity with the boronic acids can induce the deaggregation more efficiently.

We also examined the influence of linear-chain saccharides (D-mannitol, D-sorbitol and D-xylitol), disaccharides (D-cellobiose, D-maltose, D-lactose, D-palatinose and D-saccharose) and a trisaccharide (D-raffinose) on the absorption spectra of **4** in water, expecting that their complexes may be more hydrophilic than the complexes with four above-mentioned monosaccharides. As shown in Figure 10, the Soret band increases in the presence of the linear-chain saccharides

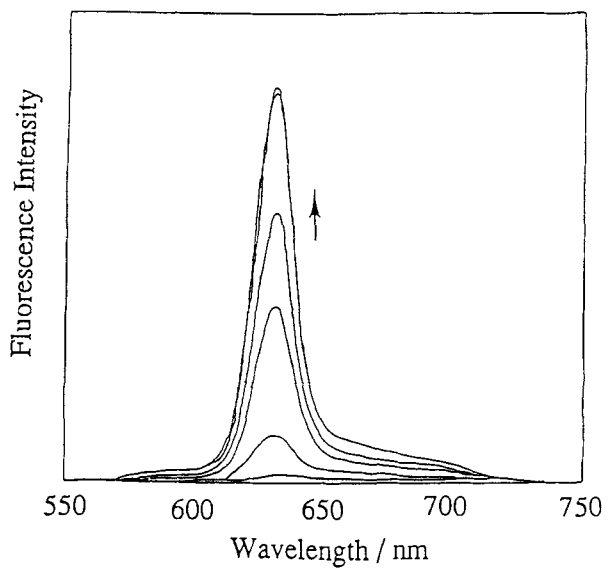

Figure 8 Fluorescence spectral change induced by the addition of D-fructose: [**4**] = 1.00×10^{-5} M, DMSO:water = 1:30 v/v, pH 10.5 with 0.067 M carbonate, 25°C, excitation 415 nm (isosbestic point in Fig. 2). In a preliminary communication (recoreded as a footnote in the first page) the wavelength in abscissa erroneously shifts by 100 nm.

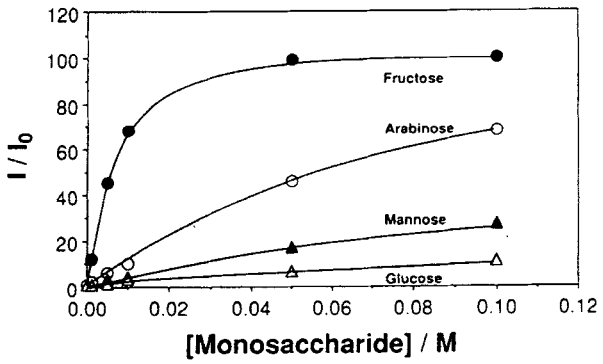

Figure 9 Fluorescence intensity at 632 nm plotted against monosaccharide concentrations. The measurement conditions are recorded in a caption to Figure 8.

but the spectral change occurs nonselectively. Disaccharides and a trisaccharide (D-raffinose) are mostly ineffective (except D-palatinose). D-cellobiose and D-maltose are dimers of D-glucose and D-lactose is a dimer composed of D-glucose and D-galactose. As mentioned above, the binding ability of D-glucose is relatively weak. D-galactose also shows weak binding comparable with D-glucose. Hence, these disaccharides should be bound to the boronic acids to a smaller extent than monosaccharides. D-saccharose and D-raffinose have a D-glucose unit and a furanose unit without a *cis*-diol. These structures also show the weak affinity with the boronic acids. In contrast, D-palatinose significantly strengthened the Soret band (Figure 10). The affinity with the diboronic acids is ascribed to the furanose unit included in D-palatinose. These results indicate that if the sugar unit which has the large affinity with boronic acids is included as a terminal unit, oligosaccharides can dissociate the aggregate and change the spectrum.

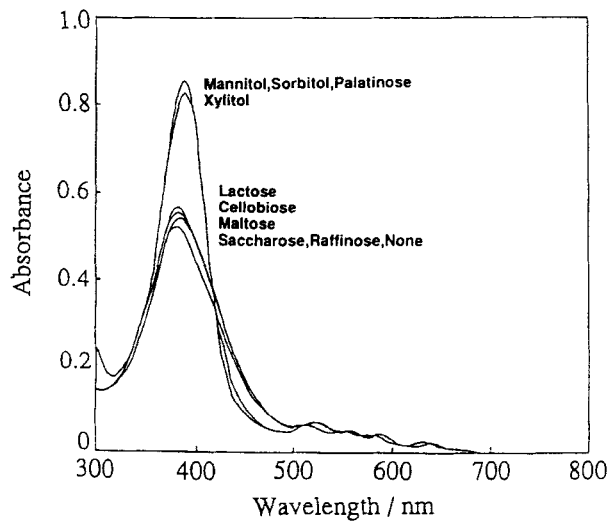

Figure 10 Absorption spectra of **4** (1.00×10^{-5} M) in the presence of linear-chain saccharides, disaccharides and a trisaccharide (0.10 M) in water. The measurement conditions are recorded in a caption to Figure 8.

Chirality of porphyrin helical aggregates is controlled by saccharides[22]

Protoporphyrins covalently-linked to glucosamine form fibrous aggregates with a chiral helical structure.[35] The results suggest that aggregates formed from boronic-acid-appended porphyrins may be orientated in a chiral manner in the presence of sugars. As a result, the absolute configuration of added sugars may be '*read out*' through the sign of the CD (circular dichroism) spectra. With these objects in mind, we synthesized a boronic-acid-appended porphyrin **5**.

Firstly, we confirmed by spectroscopic methods if **5** aggregates in aqueous solution. Compound **5** gave a sharp Soret band in DMSO (λ_{max} 427 nm) and water:DMSO = 30:1 v/v at pH 10.5 (λ_{max} 421 nm) but a broadened Soret band in water:DMSO = 30:1 v/v at pH 6.9 (λ_{max} 421 nm). The pK_a of boronic acids is estimated to be *ca.* 8.9 by photometric titration. Hence, the spectral data reveal that **5** exists discretely when the boronic acids are dissociated, whereas **5** forms aggregates when the boronic acids are undissociated. This difference was further corroborated by fluorescence spectroscopy. Although the strong fluorescence emission (λ_{EX} 433 nm, λ_{EM} 657 nm) was observable at pH 10.5, it almost disappeared at pH 6.9. The difference can be accounted for by a pH-dependent shift of an aggregation-deaggregation equilibrium in **5**. When D-arabinose, D-galactose or D-mannose was added to a solution of **5** at pH 6.9, the fluorescence intensity increased only slightly. On the other hand, a relatively large increase was observed when D-fructose was added. The fluorescence intensity increased in the order of D-fructose>> D-arabinose>D-galactose>D-mannose>D-glucose. Since this order is in line with the order of the association constant between phenylboronic acid and monosaccharides one can consider that complexation of the boronic acids with monosaccharides makes **5** more hydrophilic and induces partial dissociation of the aggregates.

The main purpose of the present study is to *read out* the absolute configuration of monosaccharides through the sign of the exciton-coupling band (ECB). The appearance of ECB is expected when **5** aggregates in solution because the exciton-coupling is a phenomenon related to the dipole-dipole interaction in the excited state. To suppress the monosaccharide-induced deaggregation we carried out the CD spectral measurement at [**5**] = 1.00 mM (for measurement conditions see Table 2). When D-fructose (0.50 M) was added, the solution of **5** was almost CD-silent. On the other hand, when other monosaccharides (0.50 M) listed in Table 2 were added, it became CD-active. The spectral parameters are sum-

Table 2 CD spectral parameters[a]

Monosaccharides	Medium[b]	λ_{max} or λ_{min} (nm) ([θ]) (deg cm^2 dmol^{-1})			Configuration of binding-sites		
					1,2[c]	3,4	4,6[d]
D-Xylose	A	433 (+1.8 × 10^4)	414 (-1.6 × 10^4)		Down/*cis*	—	—
Methyl-α-D-glucoside	A	433 (+5.6 × 10^3)	417 (-3.6 × 10^3)		—	—	Down/*trans*
D-Glucose	A	430 (+1.7 × 10^4)	414 (-2.1 × 10^4)		Down/*cis*	—	Down/*trans*
D-Talose	B	436 (-1.5 × 10^4)	420 (+3.8 × 10^4)	402 (-1.6 × 10^4)	Up/*cis*	Up/*cis*	Up/*cis*
D-Galactose	B	439 (-3.7 × 10^4)	420 (+3.1 × 10^4)	399 (-5.0 × 10^3)	Down/*cis*	Up/*cis*	Up/*cis*
D-Mannose	B	425 (-3.8 × 10^3)	412 (+3.2 × 10^3)		Up/*cis*	—	Down/*trans*
D-Ribose	A	443 (+1.5 × 10^4)	432 (-2.8 × 10^4)	417 (+2.9 × 10^4)	Down/*cis*	Down/*cis*	—
D-Arabinose	B	435 (-2.2 × 10^3)	422 (+3.2 × 10^3)	415 (+1.4 × 10^3)	Up/*cis*	Down/*cis*	—

[a][5] = 1.00 × 10^{-3} M, [monosaccharide] = 0.50 M, 25°C. [b]A, water:DMSO = 5:2 v/v; B, water:DMSO = 6:1 v/v. The water used for the preparation of mixed solvents is buffered to pH 6.9 with 0.10 M phosphate. [c]'Up' or 'down' is governed by the direction of 2-OH. [d]'Up' or 'down' is governed by the direction of 4-OH.

marized in Table 2. The solvent composition was chosen so that the exciton-coupling bands can appear distinctly. In general, a monosaccharide with a large association constant required a low DMSO concentration.

When boronic acids form complexes with monosaccharides, the binding-site is selected according to several rules.[9–30] Firstly, when a five-membered ring is formed with 1,2-diol or 3,4-diols, the *cis*-configuration is favoured. Secondly, when a six-membered ring is formed with 4,6-diols, both *cis* and *trans* can form the complexes. However, the spatial position of Ar in $ArB(OH)_2$ is governed by the configuration of 4-OH. Thirdly, the effective configuration of 1-OH for complexation is *cis* to 2-OH. Based on these rules one can summarize the possible binding-sites in monosaccharides as in Table 3, where 'up' and 'down' denote that the OH groups are placed upwards and downwards, respectively, relative to the pyranose ring. In D-xylose the sole binding-site is *cis*-1,2-diol and the **5**·D-xylose complex results in a positive ECB with a positive first Cotton effect and a negative second Cotton effect. In methyl-α-D-glucoside the sole binding site is *trans*-4,6-diol and the **5**·methyl-α-D-glucoside complex results in a positive ECB. The CD spectrum for the **5**·D-xylose complex is stronger than that for the **5**·methyl-α-D-glucoside complex. The findings suggest that (i) when 'down'-*cis*-1,2-diol or 'down'-*trans*-4,6-diol is bound to **5**, the dipoles of **5** in the aggregate cross in the (*R*)-chirality (clockwise direction); (ii) as 'down'-*cis*-1,2-diol and 'down'-*trans*-4,6-diol give a positive ECB, it is expected that enantiomeric 'up'-*cis*-1,2-diol and 'up'-*cis*-4,6-diol give a negative ECB, and (iii) when 1,2-diol and 4,6-diol give the opposite CD sign, the CD sign for 1,2-diol dominates over that for 4,6-diol but the CD intensity is weakened. From these considerations, it is readily understandable that D-glucose with 'down'-*cis*-1,2-diol and 'down'-*trans*-4,6-diol as the binding-sites gives a strong positive ECB. On the other hand, D-mannose has 'up'-*cis*-1,2-diol giving a negative ECB and 'down'-*trans*-4,6-diol giving a positive ECB. As pointed out in (iii), the former predominates over the latter. In fact, the **5**·D-mannose complex gives rise to a weak negative ECB. The rules can be extended to other monosaccharides: a strong negative ECB for D-talose with 'up'-*cis*-1,2-diol and 'up'-*trans*-4,6-diol, a positive ECB for D-ribose with 'down'-*cis*-1,2-diol and a negative ECB for D-arabinose with 'up'-*cis*-1,2-diol. Only one exception is D-galactose: from the above-mentioned rules it should give a weak positive ECB but actually, a weak negative ECB was observed.[36]

D-Talose, D-galactose, D-ribose and D-arabinose gave a second ECB at shorter wavelength region. This ECB was observed only for such monosaccharides that possess *cis*-3,4-diol. Therefore, it seems reasonable to assign

Table 3 Correlations between the absolute configuration of monosaccharides and the sign of exciton-coupling bands

Configuration		Sign of exciton-coupling at 420-440 nm	Configuration	Sign of exciton-coupling at 400-420 nm
Cis-1,2-diol	*Cis/trans*-4,6-diol		*Cis*-3,4-diol	
Down	—	Positive	Up	Positive
—	Down	Positive	Down	Negative
Up	—	Negative		
(—	Up)	(Negative)[a]		
Down	Down	Positive		
Up	Up	Negative		
Up	Down	Negative		
Down	Up	(?)[b]		

[a] It is surmised that this configuration gives a negative ECB but we could not procure the sample. [b] We expected that this configuration gives a positive ECB but D-galactose gave a weak negative ECB.

this band to complexation between **5** and 3,4-diol. Here again, one can recognize a correlation between the configuration and the CD sign: D-talose and D-galactose with 'up'-*cis*-3,4-diol give a positive ECB whereas D-ribose and D-arabinose with 'down'-*cis*-3,4-diol give a negative ECB.

DIBORONIC ACIDS

Selective binding with diboronic acids[11–13]

The diboronic acid compound **6** forms 1:1 complexes with mono- and disaccharides and gives CD (circular dichroism) spectra specific to each saccharide. It was shown on the basis of ^{1}H NMR spectroscopy that the complex with D-glucose is a macrocyclic compound formed by the reaction of the two boronic acids with *cis*-1,2-diol and *trans*-4-OH·5-CH_2OH. Thus, **6** becomes CD-active because of asymmetric immobilization of the two chromophoric benzene rings by ring closure with chiral saccharides. The association constants were in the order of D-glucose (19000 dm^3 mol^{-1}) D-talose>D-galactose>D-mannose>D-fructose (≈0 dm^3 mol^{-1}) for monosaccharides and D-maltose (100 dm^3 mol^{-1})>D-cellobiose>D-lactose>D-saccharose (≈ 0 dm^3 mol^{-1}) for disaccharides (Table 4 and 5). In particular, **6** showed very high affinity towards D-glucose. D-Glucose gave a CD spectrum with the positive exciton coupling whereas L-glucose gave a CD spectrum with the negative exciton coupling (Figure 11). D-Galactose gave a CD spectrum with the negative exciton coupling whereas all other D-mono- and D-disaccharides tested herein gave the CD spectra with the positive exciton coupling. The results indicate that the absolute configuration of saccharides can be conveniently predicted from the sign and the strength of the CD spectra of **6**. This means that the CD spectroscopic method using **6** as a receptor probe serves as a new sensory system for sugar molecules.

Compound **7** was designed for disaccharides, since the spacing between the two boronic acid units is similar to the spacing between the 1,2 -diol and 4'-OH and 5'-OH of disaccharides. In the presence of D-maltose a distinct CD band appeared (Figure 12). The split CD band which crosses the [ω] = 0 line at 210nm (λ_{max} = 207 nm in the absorption spectrum) is ascribed to exciton coupling. The negative sign for the first Cotton effect (223 nm) and the positive sign for the second Cotton effect (201 nm) indicate that the two dipoles along the phenylboronic acid molecular axis are oriented in a chiral, anti-clockwise direction when they interact in the excited state.[37] These findings reveal that when **7** forms a complex with D-maltose, the two dipoles favorably adopt (S)-chirality. Very interestingly, D-cellobiose induced the positive sign for the first Cotton effect whereas D-lactose induced the negative sign for the first Cotton effect although the maximum (or minimum) wavelength for the second Cotton effect could not be determined precisely because of the strong background noise.[38] The results imply that the complexes with D-Cellobiose and D-lactose employ (R)- and (S)-chirality, respectively. On the other hand, D-Saccharose was totally CD-silent. Because of the difficulty in the 'fine-tuning', the distance between the two boronic acids is slightly shorter than that between 1,2-diol and 4'-OH·5'-CH_2OH in disaccharides. We expected that **7** would scarcely show affinity toward monosaccharides. Contrary to our expectation, D-glucose and D-galactose behaved as CD-active monosaccharides although the [θ] values were smaller by one order of magnitude than those for disaccharides. D-Mannose and D-fructose were CD-silent. We estimated stoichiometry and association con-stants of these complexes from plots of θ vs. [disaccharide]. The results

Table 4 Absorption and CD maxima of **6**·monosaccharide complexes[a]

Saccharide	UV	CD		Stoichiometry	K[c]
	λ_{max} (nm)	λ_{max} (nm)	$[\theta]_{max}$[b] (deg cm^2 $dmol^{-1}$)		(dm^3 mol^{-1})
D-glucose	274	275	-5300	1:1	19000
		205	+231000		
	200	190	-214000		
D-mannose	272	274	-400	1:1	60
		205	+69000		
	200	191	-23000		
D-galactose	273	276	+410	1:1	2200
		205	-22000		
	200	191	+19000		
D-talose	272	275	-3700	1:1	4600
		205	+247000		
	200	190	-196000		
D-fructose	274	Nd[c]	Nd[c]	—	—
	200	Nd[c]	Nd[c]		

[a]25°C, [6] = 1.00 or 2.00 × 10^{-3} mol dm^{-3}, pH 11.3 with 0.10 mol dm^{-3} carbonate buffer. [b]$[q]_{max}$ values are calculated the 100% complex from the concentration dependence for the 1:1 complex region. [c]Nd denotes that the perceptible CD band does not appear.

Table 5 Absorption and CD maxima of **6**·disaccharide complexes[a]

Saccharide	UV	CD		Stoichiometry	*K*
	λ_{max} (nm)	λ_{max} (nm)	$[\theta]_{max}$[b] (deg cm^2 dmol^{-1})		(dm^3 mol^{-1})
D-maltose	274	275	-2400	1:1	100
		204	[4000		
	200	190	-71000		
D-cellobiose	274	275	-2000	1:1	80
		205	+39000		
	200	190	-36000		
D-lactose	274	275	-1200	1:1	15
		205	+101000		
	200	190	-60000		
D-saccharose	274	Nd[c]	Nd[c]	—	—
	200	Nd[c]	Nd[c]		

[a]Measurement conditions are recorded in a footnote to Table 4. [b]$[\theta]_{max}$ values are calculated the 100% complex from the concentration dependence for the 1:1 complex region. [c]Nd denotes that the perceptible CD band does not appear.

Table 6 Absorption and CD spectra of **7** and its disaccharide complexes and their ass constants (K)[a]

Disaccharide	Absorption maximum nm	CD maximum	K
	nm	λ ([θ]) nm(deg cm^2 dmol^{-1})	dm^3 mol^{-1}
D-maltose	207	223 (-17000) 201[b]	200
D-cellobiose	207	224 (19000) 203[c]	50
D-lactose	207	226(-4000) —[d]	400
D-saccharose	207	silent	—

[a]25°C, pH=10.5 with 0.1 mol dm^{-3} carbonate buffer. [b]$[\theta]_{max}$ is positive, but [θ] could not be determined precisely. [c]$[\theta]_{max}$ is negative, but [θ] could not be determined precisely. [d]$[\theta]_{max}$ is positive, but [θ] and λ_{max} could not be determined precisely.

are summarized in Table 6. It was found that all of the CD-active complexes with **7** have 1:1 stoichiometry. In complexation with D-maltose and D-Cellobiose the cis-1,2-diol moiety is used as the primary binding site and the trans-4'-OH·5'-CH_2OH moiety is used as the secondary binding site. Other than these, no other diol groups satisfy the requirements for complexation with boronic acids. In D-lactose, on the other hand, there are two possible secondary binding sites, cis-3',4'-diol and trans-4'-OH·5'-CH_2OH. In D-Saccharose, there is no cis-1,2-diol which can serve as a primary binding site.

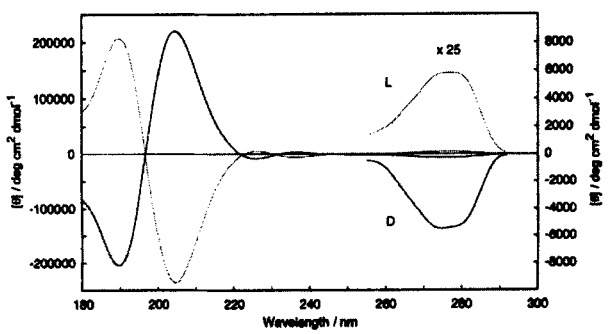

Figure 11 CD spectra of **6** in the presence of D-glucose (blue line) and L-glucose (red line): [glucose] = 2.00 × 10^{-3} mol dm^{-3}, [**6**] = 1.00 × 10^{-3} mol dm^{-3}, pH 11.3 with 0.10 mol dm^{-3} carbonate buffer, 25°C. (See Color Plate XXI.)

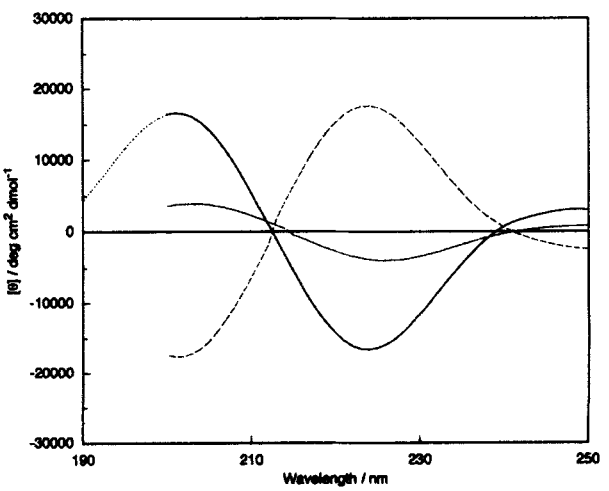

Figure 12 CD spectra of **7** in the presence of D-maltose (blue line), D-cellobiose (red line) and D-lactose (green line): [disaccharide] = 5.00 × 10^{-3} mol dm^{-3}, [**7**] = 5.00 × 10^{-3} mol dm^{-3},pH 10.5 with 0.10 mol dm^{-3} carbonate buffer, 25°C. (See Color Plate XXII.)

Allosteric Interaction of metal ions with saccharides in a crowned diboronic acid[14]

The remarkably strong interaction between the diphenylmethane-3,3'-diboronic acid **6** and glucose has shown that the design of a glucose selective pocket is possible. With the success of this molecular design we were prompted to exploit our saccharide cleft in more complex systems such as allosteric devices. Such systems should mimic the modes of sugar recognition in nature more precisely.

Synthetic allosteric devices in the past have mainly relied on metal ion coordination or lipophillic interactions.[39–49] Light has also been employed in allosteric devices to control the conformation and hence binding of diazo crowns.[50–54] In the design of an allosteric system binding at the first or main site should either activate (positive allostericity) or deactivate (negative allostericity) binding at the second site. To facilitate activation or deactivation, binding at the first site should induce a major conformational change in the molecule. From our previous work with the diphenylmethane-3,3'-diboronic acid, we know that binding of a saccharide immobilizes the two phenyls with a twist (Figure 13). This asymmetric immobilization can be readily "read-out" as a change in circular dichroism (CD) of the benzene chromophore. If the second binding site requires a different disposition of the two aromatic rings then negative cooperativity (or allostericity) will be observed; conversely if both sites align with the same disposition positive cooperativity (or allostericity) will result. One possible secondary site is a metal binding site; crown ethers are then the obvious first choice.[55] If a crown ether is employed in the molecular design then the ideal starting structure **8a, b** has the methylene bridge of **6** replaced with an oxygen. For these molecules metal binding should induce the classic "crown" of oxygens. Since this will force the phenyls into the same plane, negative cooperativity is predicted.

The change of the CD intensity of the D-allose 1:1 complex with **8b** with added metal is given in Figure 14. With the monocations of lithium, sodium, rubidium and cesium, no significant change was observed, but with potassium a significant perturbation of the D-allose binding with increasing metal ion concentration was observed. The equilibrium constant of 1180 M^{-1} decreases to a minimum of 910 M^{-1}. The dications of magnesium and calcium are both efficient in perturbing the binding of D-allose, with calcium being particularly efficient. The equilibrium constant of 1180 M^{-1} decreases to 300 M^{-1} with added calcium. In order to confirm that we are in fact observing allosterism and not some secondary effect the CD spectra of **9** in the presence of added metal were recorded. As expected, no significant change was observed with any of the metal ions tested herein.

Why do dications induce a larger negative allosterism than monocations? This question has a very simple answer. The measurements were carried out at pH 11.6 and at this pH both boronic acid groups exist as boronate anions. Thus, the electrostatic stabilization with dications is stronger than with the monocations.

Further confirmation that it is negative allosterism we are observing is given by the change in the CD intensity of D-glucose, D-talose, and D-allose 1:1 complexes on addition of calcium perchlorate. The equilibrium constants change from 31000 M^{-1} to 25400 M^{-1}, 14000 M^{-1} to 8400 M^{-1} and 1180 M^{-1} to 300 M^{-1} respectively. (Figure 15) From Table 7 the order of decreasing stability for the 1:1 complex is D-glucose D-taloseD-allose. The

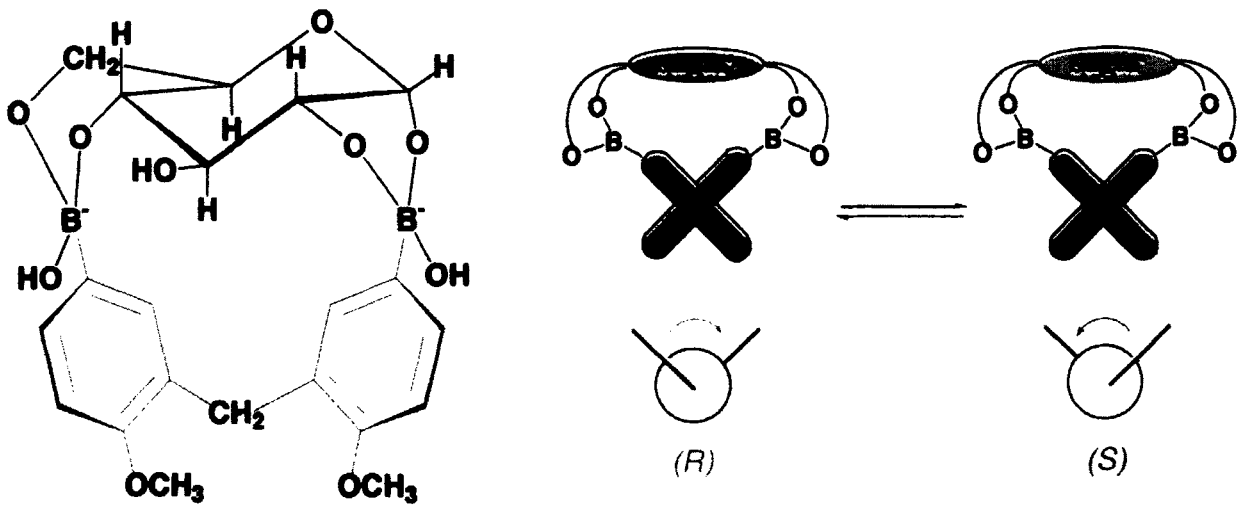

Figure 13 Proposed structure of D- glucose complex, and a pair of altropisomers. Here the pyranose form of glucose is given, but the furanose complex cannot be ruled out. (See Color Plate XXIII.)

Table 7 Absorption and CD Spectra Parameters of **8b**·Saccharide Complexes[a]

saccharide	UV	CD		stoichiometry	K^c
	λmax (nm)	λmax (nm)	[θ]max[b] (deg cm^2 dmol^{-1})		(M^{-1})
D-glucose	287	289	+32810	1:1	31000
	200	212	+245100		
		192	-432000		
D-talose	288	288	+7298	1:1	14000
	200	212	+126000		
		196	-334300		
D-allose	288	288	+3815	1:1	1180
	200	213	+107400		
		193	-251000		
D-mannose	287	silent	silent	-	-
	200	silent	silent		

[a][**8b**] = 1.63 × 10^{-3} M, pH = 11.6 with 0.2% choline hydroxide in 9:1 CH_3OH/H_2O at 25°C. [b][q]max values were calculated for 100% complexation. [c]Maximum error ±200 M^{-1}

effect of calcium on the binding of these saccharides reflects this order, since the most stable complex is the least affected by added calcium.

Chirality control of Tris (2,2'-bipyridine)-Metal Complexes[23]

Figure 16 shows the CD spectra of **10** in the presence of D-maltose ($[\theta]_{205}$ = -2900 deg cm^2 dmol^{-1}) or D-cellobiose ($[\theta]_{212}$ = 6600 deg cm^2 dmol^{-1}). It is known that **7** shows the negative exciton coupling with the negative first Cotton effect and the positive second Cotton effect in the presence of D-maltose and the positive exciton coupling with the positive first Cotton effect and the negative second Cotton effect in the presence of D-cellobiose. The coincidence between the CD sign in Figure 16 and that of the first Cotton effect in the disaccharide·**7** complexes suggest that the bands in Figure 16 correspond to the first Cotton effect in the exciton coupling.[11-13]

A plot of $[\theta]_{205}$ against D-maltose concentration is shown in Figure 17. The concentration dependence is biphasic with a $[\theta]_{205}$ minimum. Other disaccharides also showed a similar dependence. A similar concentration dependence was previously observed for **7**.[11-13]

When Fe^{2+} (added as $FeCl_2$) is added to a solution containing the disaccharide·**10** complex, the CD spectrum with an exciton coupling band appears at the metal-ligand charge-transfer (MLCT) band region (Figure 18). The same CD spectrum was produced when disaccharide was added to the solution containing the Fe^{2+}·(2,2'-bipyridine)$_3$ complex. Separately, we confirmed that the Fe^{2+}·(2,2'-bipyridine)$_3$ complex is CD silent even in the presence of disaccharides. Hence, the CD-activity is attributable to the generation of chiral

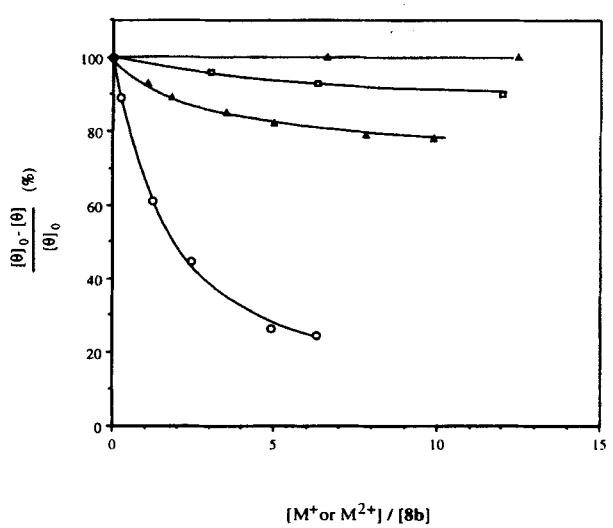

Figure 14 Decrease of the CD intensity of D-allose • **8b** complex in the presence of metal perchlorate: Ca^{2+}(O), K^+(Δ), Mg^{2+}(□), [Li^+, Na^+, Rb^+, Cs^+](▲). **8b** = 1.63 × 10^{-3} M. pH = 11.6 with 0.2% choline hydroxide as the base in 9:1 CH_3OH / H_2O at 25°C. $[\theta]_O$ and [θ] are the CD intensity in the abscence or in the presence of metal salt.

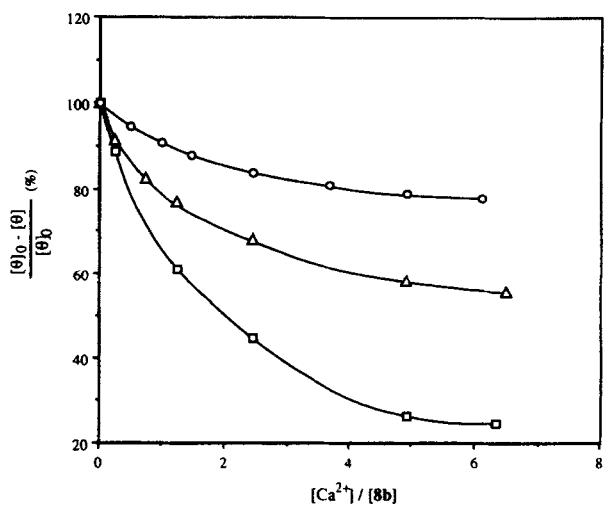

Figure 15 Decrease of the CD intensity of monosaccharide • **8b** complexes: D-glucose (O), D-talose (Δ), D-allose (□). **8b** = 1.63 × 10^{-3} M. pH-= 11.6 with 0.2% choline hydroxide as the base in 9:1 CH_3OH / H_2O at 25°C. $[\theta]_O$ and [θ] are the CD intensity in the abscence or in the presence of calcium perchlorate.

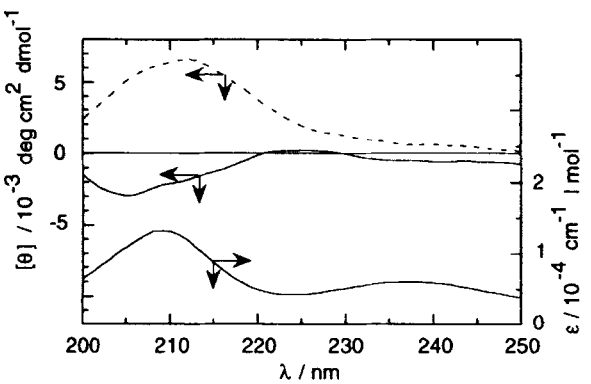

Figure 16 CD spectra of **10** (5.0 mM) in the presence of D-maltose (50 mM, _____) or D-cellobiose (50 mM, -----) and absorption spectrum of **2** (32.4 mM): 25°C, pH = 10.5.

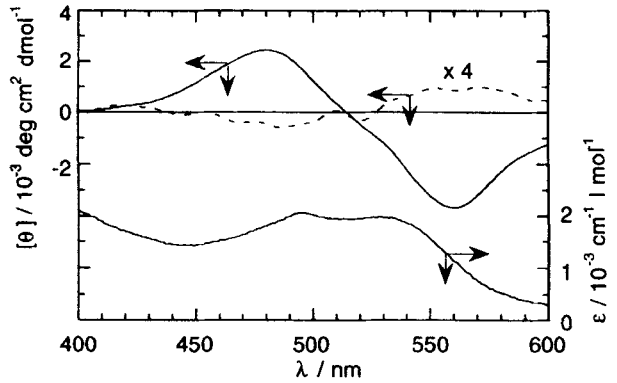

Figure 18 CD spectra of Fe^{2+}·**10**$_3$ (6.0 mM) in the presence of D-maltose (18 mM, _____) and D-cellobiose (18 mM, -----): 4°C, pH = 10.5 and absorption spectrum of Fe^{2+}·**2**$_3$ (0.5 mM): 25°C, pH = 10.5.

Fe^{2+} complexes which is originated from the disaccharide-diboronic acid interaction. Figure 18 shows that Fe^{2+}·(**10**·D-maltose)$_3$ adopts Λ chirality while Fe^{2+}·(**10**·D-cellobiose)$_3$ adopts Δ chirality.[56]

Figure 19 shows a plot of $[\theta]_{556}$ ([θ] minimum) and $[\theta]_{480}$ ([θ] maximum) at the MLCT band region *vs.* D-maltose concentration. Strangely, the MLCT band region is still CD active in the presence of excess D-maltose while **10** itself becomes CD-silent. This implies that in **10** the intramolecular cross-link of two boronic acids is indispensable to the CD-activity whereas in Fe^{2+}·(**10**·disaccharide)$_3$ it is not a prerequisite to the CD-activity.

FLUORESCENCE

Photoinduced electron transfer (PET) sensor[18]

Photoinduced electron transfer (PET) has been wielded as a tool of choice in fluorescent sensor design for protons and metal ions.[57] Design of fluorescent sensors for neutral organic species presents a harsher challenge due to the lack of electronic changes upon inclusion. The design of a fluorescent sensor based on the boronic acid saccharide interaction has been difficult due to the lack of sufficient electronic changes found in either the boronic acid moiety or in the saccharide moiety. Furthermore, facile boronic acid saccharide complexation occurs only at high pH, conditions required to create a boronate anion. It has been shown that saccharide complexation changes the pK_a of the boronic acid moiety.[25,30,32] It has been observed that 2- and 9-anthrylboronic acids display enhanced acidity upon binding to saccharides and consequent fluorescent suppression by the boronate anion *via* a photoinduced electron transfer mechanism.[25] However, the photoinduced electron transfer from the boronate anion was not efficient despite the fact that the boronate anion is directly bound to the chromophore (*I*(in the presence of saccharide)/*I*$_0$(in the absence of saccharide) = *ca.* 0.7)

In order to overcome the above mentioned disadvantages of boronic acid saccharide interactions, we have modified the boronic acid binding site to create a better electron center around the boronic acid moiety. The basic skeleton of a known PET sensor **12** has been preserved.[58] In addition, the amine can interact intramolecularly with

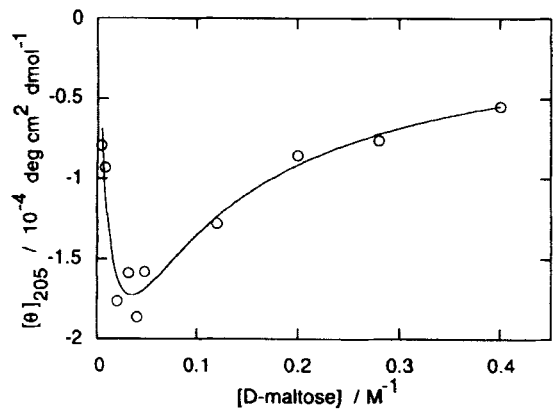

Figure 17 Plot of $[\theta]_{205}$ *vs.* [D-maltose]: 25°C, pH = 10.5, [**10**] = 5.0 mM.

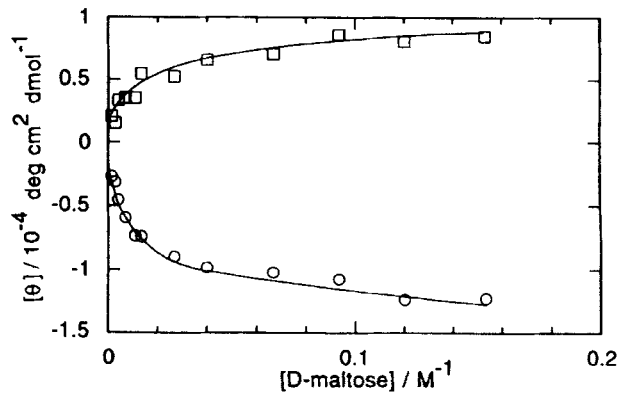

Figure 19 Plot of $[\theta]_{556}$ (O) and $[q]_{480}$ (□) *vs.* [D-maltose]: 25°C, pH = 10.5, [Fe^{2+}·**10**$_3$] = 6.0 mM.

the boronic acid, as in **13**, creating a five member ring. The fluorescence pH profile of **11**, in unbuffered aqueous media, as given in Figure 20, gave one large step at low pH (pK_a = 2.9) and a possible small step at high pH. The pK_a of **12** is known to be 9.3 (fluorescence measurements in ethanolic aqueous media).[58] The large shift of the pK_a is due to the interaction found between the boronic acid moiety and the amine group. However, the boronic acid-amine interaction does not inhibit the photoinduced electron transfer quenching process in the complex **11b** (scheme 3). Complete separation of the amine and the boronic acid moiety at very high pH, as in **11c**, further quenched the anthracene fluorescence. However, the fluorescence decrease is insufficient for the calculation of the pK_a. The introduction of saccharides (D-glucose and D-fructose) remarkably changes the fluorescence of **11** over a large pH range (Figure 20). Scheme 3 is suggestive of the most important species involved in the fluorescence changes. The enhanced interaction between boronic acid and amine, upon saccharide binding, inhibits the electron transfer process giving greater fluorescence (as **11d** in scheme 3). This increased interaction would be expected since the saccharide binding to boronic acid increases its acidity creating a more electron deficient boron atomic center. The two saccharides studied gave similar fluorescence enhancements. More flexible and less bulky ethylene glycol gave very low fluorescence enhancements, suggesting the importance of some steric factors. The pK_a for the saccharide complex, as calculated from fluorescence measurements at high pH (pK_a = 11.1), is in line with the second pK_a of **13** in the absence of sugar (pK_a = 11.8)[30] which is the parent binding site of **11**. However, no significant difference was found between fructose and glucose. From these fluorescent measurements we could not estimate the first pK_a of the saccharide-**11** complex due to insufficient changes in fluorescence intensities.

Rigidification and Fluorescence Enhancement of Stilbene diboronic acids[24]

The diboronic acids **6** and **7** form rigid cyclic complexes with mono- and disaccharides. The induced chirality upon formation of rigid, chiral complexes was monitored by CD spectroscopy. This regidification process can be utilized in the design of spectroscopic sensors. The main path of nonradiative deactivation of the lowest excited singlet state of stilbene is known to be *via* rotation of the ethylenic double bond.[59] Inhibited bond rotation, followed by enhanced fluorescence emission has been reported for stilbenes in solid matrices[59], viscous solvents[60] and cyclodextrin inclusion complexes.[61]

The fluorescence of stilbene-3,3'-diboronic acid **14** increases upon binding to disaccharides in basic aqueous media. Figure 21 shows the fluorescence intensity and the saccharide concentration profiles for **14**. Large fluorescence increases were observed specifically for the

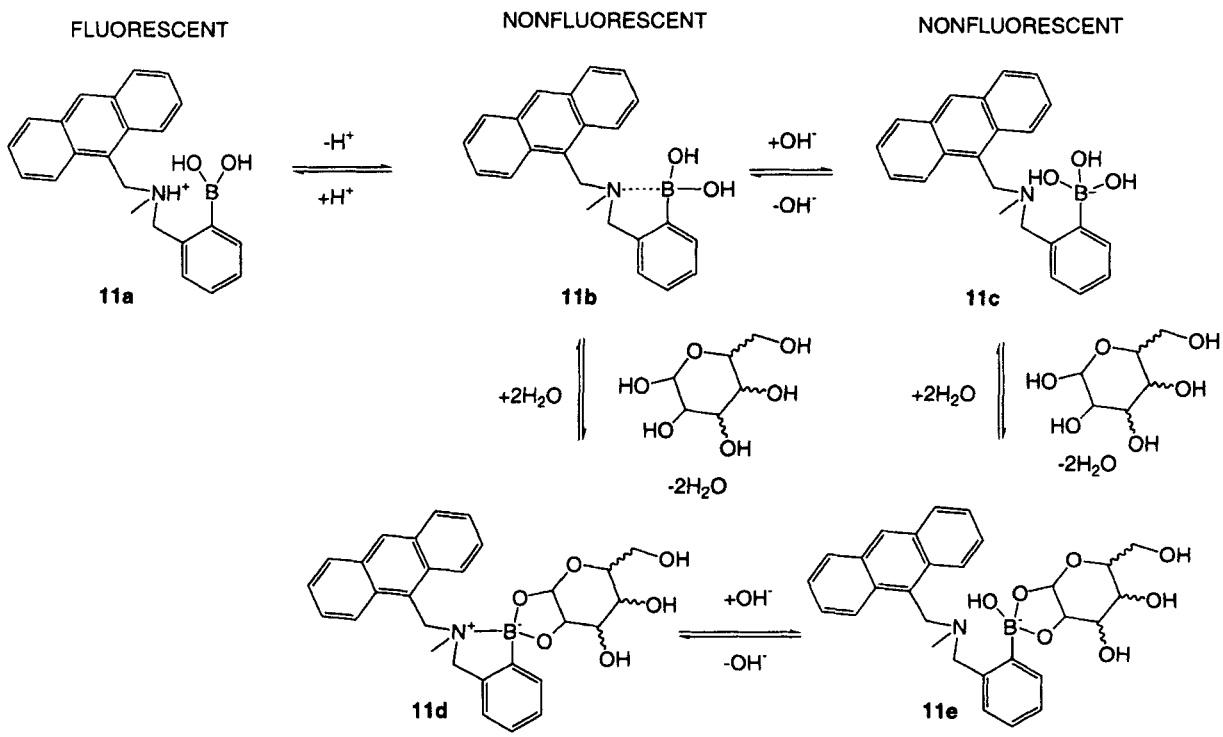

Scheme 3

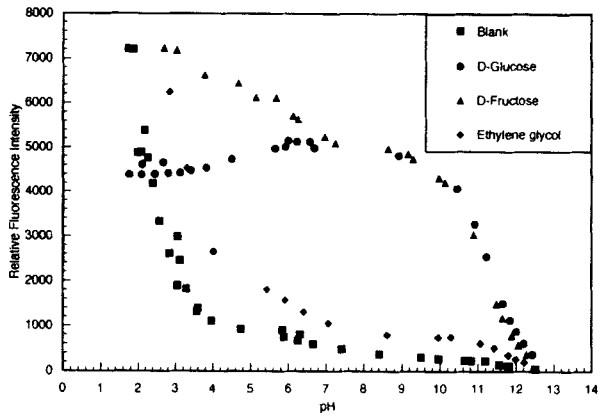

Figure 20 Fluorescence intensity pH profile of **11** at 25°C; 1.2×10^{-5} M of **11** in 0.05M sodium chloride solution, [saccharide or ethylene glycol] = 0.05M.

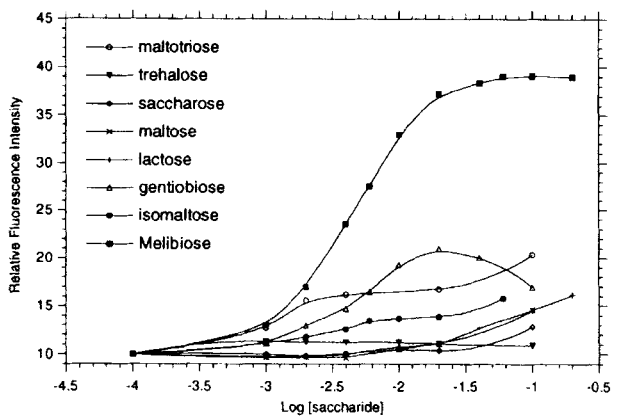

Figure 21 Fluorescence titration of stilbene diboronic acid **14** (1.0×10^{-5} M) at pH 10.6 (0.1 M sodium carbonate / sodium bicarbonate buffer) as a function of log of disaccharide concentration (ex. 310 nm, em. 358 nm)

disaccharide D(+)-melibiose in basic aqueous media compared to small increases observed for monosaccharides (D(+)-glucose, D(+)-mannose and D(-)-arabinose) (Figure 21). This fluorescence increase was attributed to the formation of a cyclic complex of diboronic acid with disaccharide and subsequent freezing of ethylenic bond rotation in the excited state (Scheme 4).[62]

It has been established that phenylboronic acid binding to monosaccharides in basic aqueous media occurs primarily at 1,2-diols and secondary binding at 4,6-diols creating five and six membered rings respectively[3]. The hydroxyl group at the 3 position does not participate in complexation, as it has been proved by complexation of boronic acid with glucose derivatives[9–30]. Diboronic acids **6** and **7** formed cyclic, CD active complexes with saccharides. It was shown that the cyclic complex formed in aqueous media with saccharides employs the same binding sites as the 1:2 complex formed with monoboronic acid[9–30] i.e. 1,2- and 4,6-diols participate in complexation creating a cyclic complex and the 3 hydroxy group plays no part in the complexation process. D(+)-melibiose, which has 4,6-*cis*- and possible 1',2'-*cis*- diols in aqueous media, gave the best fluorescence enhancement whereas the disacharide gentiobiose, which has 4,6-*trans* and 1',2'-*cis*-diols, gave somewhat less fluorescence enhancements. Gentiobiose suppressed the fluorescence at high concentrations, possibly due to competitive 1:2 complex formation. Isomaltose which has a 1,6'-ether link between sugar monomers, (as does melibiose and gentiobiose) gave small fluorescence enhancements. It seems that among these three disaccharides, which have 1,6'-ether links between sugar monomers, D(+)-melibiose has the best fit for the diboronic acid receptor. Maltose, which has a 1,4'-ether link between saccharide monomers did not give any fluorescence enhancement although, interestingly, maltotriose which has an extended monomer unit gave some fluorescence enhancement. Other disaccharides studied which have shorter distances between prospective diol groups gave no fluorescence enhancements. This suggests the length of the disaccharide is important.

LIQUID CRYSTALS

Cholesterylboronic acid complexes of monosaccharides alter the colour of a composite chiral cholesteric liquid crystal membrane, the direction of the visible colour change being indicative of the absolute configuration of the monosaccharide.

Solvent extraction of saccharides with **15** was carried out at 25°C using solid-liquid ($CDCl_3$) extraction. The induced shifts produced by the extracted monosaccharides in a cholesteryl chloride/nanoate composite liquid crystal[63] are given in Table 8.

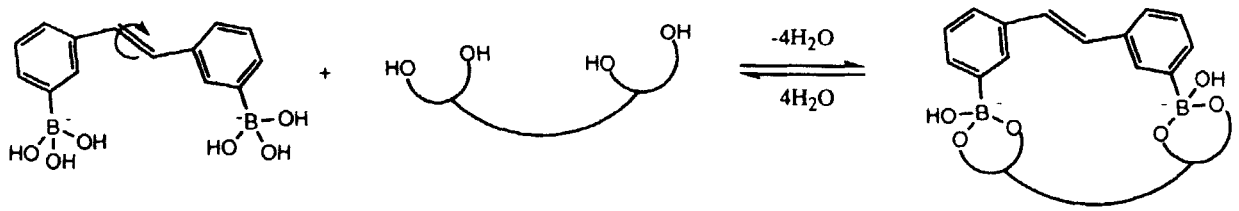

Scheme 4

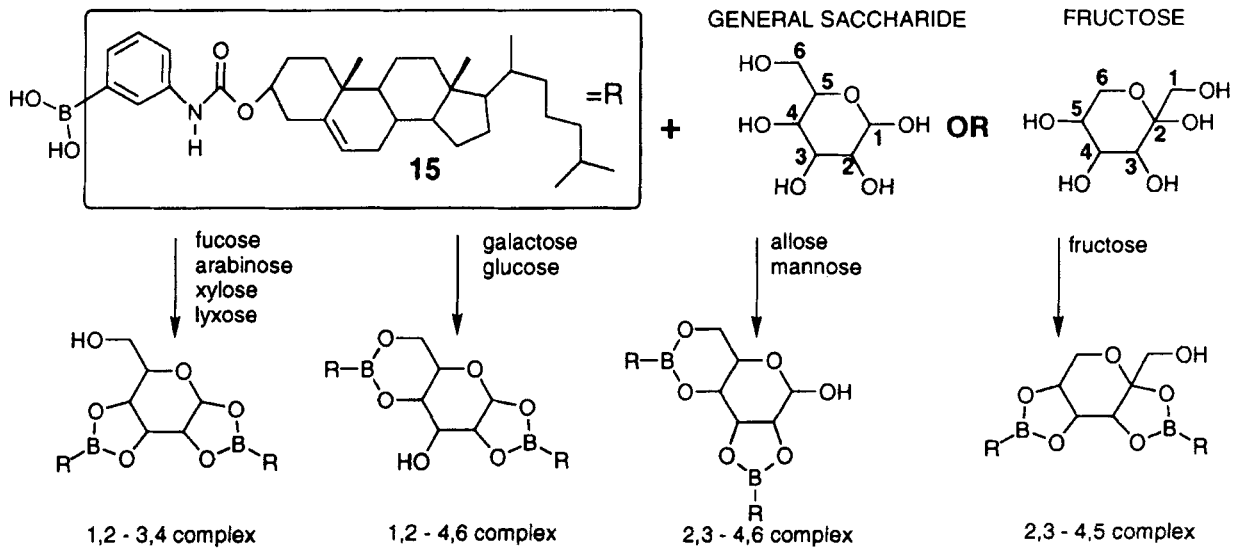

Figure 22 Structures of 2:1 complexes (**15**/monosaccharide).

Analysis of Figure 22 and Table 8 shows that saccharides with similar structural features induce shifts in the same sense (Figure 23). With the saccharides extracted three such structure/shift group relationships exist. The first group includes saccharides with two (*cis*) five membered boronate ester rings (Group I). When the first ring (following normal saccharide numbering) is down with respect to the saccharide plane and the second is up, a red shift is induced (D-fucose, L-arabinose). Conversely, when the first ring is up and the second is down, a blue shift is induced (D-fructose, D-arabinose, L-fucose). The next structure/shift sub-group contains saccharides with one *cis* five membered ring and either a *trans* five or a *trans* six membered *trans* ring (Group II). When the first ring (*cis* five membered) is down a red shift is induced (D-glucose, D-allose, D-xylose), and conversely when this ring is up a blue or no shift is induced (L-glucose, D-mannose). The final structure/shift group is the most anomalous; the saccharide contains both a *cis* five membered ring and *cis* six membered ring (Group III). When the first ring is either up or down a blue shift is induced (D-galactose, L-galactose), D-tallose induces no shift. This anomalous behaviour may be a result of the conformational lability of the *cis* six membered ring, or as explained below, the behaviour may not be anomalous if a threshold must be overcome before a shift in the pitch occurs.

From the above qualitative structural analysis and the result that the 1:1 complex of 2-deoxy-D-galactose causes no shift, it seems that the spatial disposition of two cholesteryl boronic acid moieties is the driving force for the change in the cholesteric pitch. Structural analysis of the complexes utilising a molecular orbital calculation[64–66] reveals a quantitative relationship between the

Table 8 Shifts in the reflectance maxima caused by added 2:1 complex: **15**/saccharide

Group	2:1 Complex **15**/saccharide	Induced shift[a] relative to compound **15**	
		mol% 2.4[b]	mol% 1.2[c]
	D-fucose		123±13
	L-arabinose		27±8
I	L-fucose	-164±12	-95±6
	D-arabinose	-82±10	-45±6
	D-fructose	-37±11	-23±11
	D-glucose	91±10	42±12
	D-allose	69±10	19±10
II	D-xylose		34±15
	L-glucose	-71±10	-61±6
	D-mannose	-3±10	5±6
	D-galactose	-44±10	-33±11
III	L-galactose	-17±10	-21±7
	D-talose	3±11	
Blank	2-deoxy-D-galactose	6±15	

[a]Shifts are the average of five repeats, errors given are the maximum deviation from the mean. [b]At 2.4mol% compound **15** has a base reflectance of 625±10. [c]At 1.2mol% compound **15** has a base reflectance of 650±6.

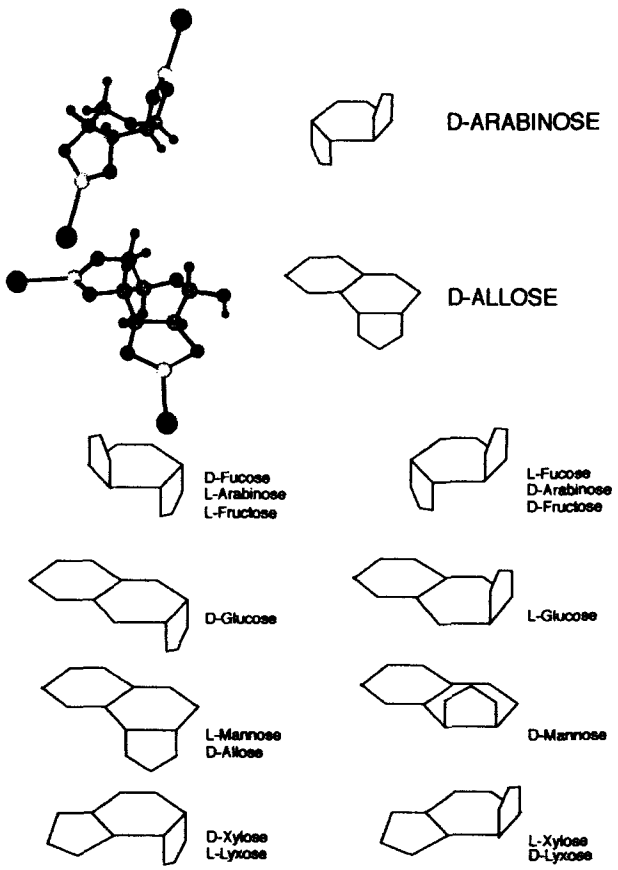

Figure 23 Cartoon representation of 2:1 complex, with two calculated structures for comparison. (See Color Plate XXIV.)

magnitude and direction of the induced shift and the angle between the phenyl planes of the two boronic acid moieties (Figure 24). For the correlation depicted in Figure 24, one apparent anomaly needs to be clarified. Why are blue shift additives "effective" at all angles, but those compounds inducing a red shift have a threshold value of about 40° (D-fructose)? This can be explained by the inherent twist of the support liquid crystal; complexes that add to this inherent twist cause blue shifts, and those that subtract cause red shifts, with D-fructose (40°) acting as the effective zero or threshold.

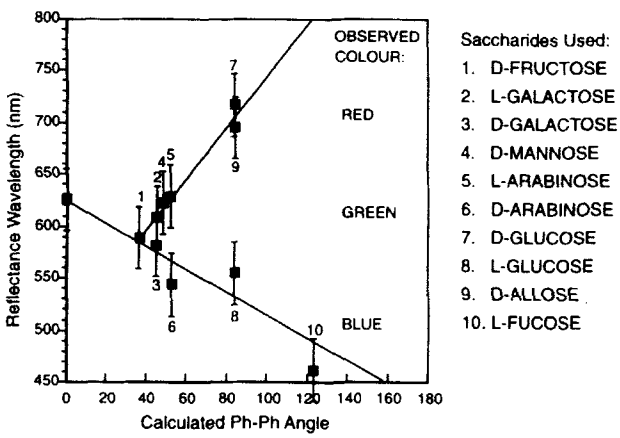

Figure 24 Plots of reflectance wavelength *vs.* calculated ph-ph dihedral angle for 2:1 complex.

REFERENCES

1 Elsaa, L. J.; Rosenberg, L. E. *J. Clinic. Invest.* **1969**, *48*, 1845.
2 De Marchi, S.; Cecchin, E.; Basil, A.; Proto, G.; Donadon, W.; Jengo, A.; Schinella, D.; Jus, A.; Villalta, D.; De Paoli, P.; Santini, G.; Tesio, F. *Am. J. Nephrol.* **1984**, *4*, 280.
3 Baxter, P.; Goldhill, J.; Hardcastle, p. T.; Taylor, C. J. *Gut.* **1990**, *31*, 817.
4 Yasuda, H.; Kurokawa, T.; Fuji, Y.; Yamashita, A.; Ishibashi, S. *Biochim. Biophys. Acta.* **1990**, *1021*, 114.
5 Fedoak, R. N.; Gershon, M. D.; Field, M. *Gasteroenterology* **1989**, *96*, 37.
6 Yamamoto, T.; Seino, Y.; Fukumoto, H.; Koh, G.; Yano, H.; Inagaki, N.; Yamada, Y.; Inoue, K.; Manabe, T.; Imura, H. *Biochem. Biophys. Res. Commun.* **1990**, *170*, 223.
7 For a recent comprehensive review see S. Misumi, *Kagaku To Kogyo* (*Chem. Chem. Ind.*) **46**, 756 (1993).
8 Goto, T.; Kondo, T. *Angew. Chem. Int. Ed. Engl.* **30**, 17 (1991).
9 Shinkai, S.; Tsukagoshi, K.; Ishikawa, Y.; Kunitake, T. *J. Chem. Soc., Chem.Commun.* **1991**, 1039.
10 Tsukagoshi, K.; Shinkai, S. *J. Org. Chem.* **1991**, *56*, 4089.
11 Kondo, K.; Shiomi, Y.; Saisho, M.; Harada, T.; Shinkai. S. *Tetrahedron* **1992**, *48*, 8239.
12 Shiomi, Y.; Kondo, K.; Saisho, M.; Harada, T.; Tsukagoshi, K.; Shinkai, S. *Supramolecular. Chem.* **1993**, *2*, 11.
13 Shiomi, Y.; Saisho, M.; Tsukagoshi, K.; Shinkai, S. *J. Chem. Soc. Perkin Trans. 1* **1993**, 2111.
14 Deng, G.; James, T. D.; Shinkai, S. *J. Am. Chem. Soc.* **1994**, *116*, 4567.
15 James, T. D.; Harada, T.; Shinkai, S. *J. Chem. Soc., Chem. Commun.* **1993**, 857 and 1176 (corrigendum)
16 James, T. D.; Murata, K.; Harada, T.; Ueda, K.; Shinkai, S. *Chem. Lett.* **1994**, 273.
17 Ludwig, R.; Harada, T.; Ueda, K.; James, T. D.; Shinkai, S. *J. Chem. Soc, Perkin Trans. 2* **1994**, *4*, 697.
18 James, T. D.; Sandanayake, K. R. A. S; Shinkai, S. *J. Chem. Soc., Chem. Commun.* **1994**, 477.
19 Sandanayake, K. R. A. S.; Shinkai, S. *J. Chem. Soc., Chem. Commun.* **1994**, 1083.
20 Nagasaki, T.; Shinmori, H.; Shinkai, S. *Tetrahedron Lett.* **1994**, 2201.
21 Murakami, H.; Nagasaki, T.; Hamachi, I.; Shinkai, S. *J. Chem. Soc., Perkin Trans.* 2 **1994**, 975.
22 Imada, T.; Murakami, H.; Shinkai, S. *J. Chem. Soc., Chem. Commun.* **1994**, 1557.
23 Nakashima, K.; Shinkai, S. *Chem. Lett.* **1994**, 1267.
24 Sandanayake, K. R. A. S.; Nakashima, K.; Shinkai, S. *J. Chem. Soc., Chem. Commun.* **1994**, 1267.
25 Yoon, J.; Czarnik, A. W. *J. Am. Chem. Soc.* **1992**, *114*, 5874.
26 Mohler, L. K.; Czarnik, A. W. *J. Am. Chem. Soc.* **1993**, *115*, 7037.
27 Mohler, L. K.: Czarnik, A. W. *J. Am. Chem. Soc.* **1993**, *115*, 2998.
28 Wulff, G.; Heide, B.; Helfmeier, G. *J. Am. Chem. Soc.* **1987**, *108*, 1089.
29 Wulff, G.; Poll, H.-G. *Makromol. Chem.* **1987**, *188*, 741
30 For a comprehensive review see Wulff, G. *Pure Appl. Chem.* **1982**, *54*, 2093.
31 From our work and that of others (references 9–30) it is known that the boronate ester is rapidly and reversibly formed under basic conditions. Noncovalent interactions are described using such terms as "recognition", "complex" and "binding constants". These terms will be used to describe the equilibrium between covalent boronate ester and free boronic acid at high pH.
32 Lorand, J. P.; Edwards, J. D. *J. Org. Chem.* **1959**, *24*, 769.

33 K. Yoshino, M. Fukuda, and Y. Mori, Paper presented at the 58th Annual Meeting of the Chemical Society of Japan, **1989**, Kyoto

34 Inamura, I; Uchida, K. *Bull. Chem. Soc. Jpn.* **1991**, *64*, 2005.

35 Fuhrhop, J.-H.; Demoulin, C.; Boettcher, C.; König, J.; Siggel, U. *J. Am. Chem. Soc.* **1992**, *114*, 4159.

36 In the CD studies of monosaccharides D-galactose frequently shows exceptional behaviours.[2] The reason is not well understood. Here the discussions are made for the pyranose form but similar discussions are possible for the furanose form.

37 Harada, N.; Nakanishi, K.; *Acc. Chem. Res.* **1972**, *5*, 257.

38 The clear exciton coupling for D-lactose was observed at [D-lactose] >2.5 × 10^{-3} mol dm^{-3}

39 Rebek, J. Jr. *Acc. Chem. Res.* **1984**, *17*, 258.

40 Rebek, J. Jr.; Trend, J. E.; Wattley, R. V.; Chakravorti, S. *J. Am. Chem. Soc.* **1979**, *101*, 4333,

41 Rebek, J. Jr.; Wattley, R. V. *J. Am. Chem. Soc.* **1980**, *102*, 4853.

42 Rebek, J. Jr.; Wattley, R. V.; Costello, T.; Gadwood, R.; Marshal, L. J. *Am. Chem. Soc.* **1980**, *102*, 7400.

43 Rebek. J. Jr.; Costello, T.; Marshall, L. *J. Am. Chem. Soc.* **1983**, *105*, 6759.

44 Rebek, J. Jr.; Costello, T.; Marshall, L.; Wattley, R.; Gadwood, R. C.; Onan, K. *J. Am. Chem. Soc.* **1985**, *107*, 7481.

45 Sijibesma, R. P.; Nolte, R. J. M. *J. Am. Chem. Soc.* **1991**, *113*, 6695.

46 Gagnaire, G.; Gellon, G.; Pierre, J-L. *Tetrahedron. Lett.* **1988**, 933.

47 Beer, P. D.; Rothin, A. S. *J. Chem. Soc., Chem. Commun.* **1988**, 52.

48 Schneider, H-J.; Ruf, D. *Angew. Chem. Int. Ed. Engl.* **1990**, *29*, 1159.

49 Schneider, H-J.; Werner, F. *J. Chem. Soc., Chem. Commun.* **1992**, 490.

50 Shinkai, S.: Nakaji, T.; Ogawa, T.; Shigematsu, K.; Manabe, O. *J. Am. Chem. Soc.* **1981**, *103*, 111.

51 Shinkai, S; Nakaji, T.; Nishida, Y.; Ogawa, T.; Manabe, O. *J. Am. Chem. Soc.* **1980**, *102*, 5860.

52 Shinkai, S.; Minami, T.; Kusano, Y.; Manabe, O. *J. Am. Chem. Soc.* **1982**, *104*, 1967.

53 Shinkai, S.; Kinda, H.; Manabe, O. *J. Am. Chem. Soc.* **1982**, *104*, 2933.

54 For a comprehensive review see Shinkai, S. In *Cation Binding by Macrocycles* (ed by Inoue, Y.; Gokel, G. W.); Marcel Dekker: New York, 1990, chapter 9.

55 Samoshin, V. V.; Zapol'skii, M. E.; Yartseva, I. V.; Zefirov, N. S. *Zh. Org. Khim.*, **1991**, *27*, 2227 and references cited therein.

56 Mason, S. F.; Peart, B. J. *J. Chem. Soc., Dalton Trans.* **1973**, 949.

57 (a) Bryan, A. J; de Silva, A. P; de Silva, S. A.; Rupasingha, R. A. D.; Sandanayake, K. R. A. S., *Biosensors* **1989**, *4*, 169. (b) Bissel, R.; de Silva, A. P.; Gunaratna, H. Q. N.; Lynch, P. L. M.; Maguire, G. E. M.; Sandanayake, K. R. A. S., *Chem. Soc. Rev.* **1992**, *21*, 187.

58 A. P. de Silva and R. A. D. D. Rupasingha, *J. Chem. Soc., Chem. Commun.* 1985, 1669.

59 Turro, N. J. Modern Molecular Photochemistry, The Benjamin, Menlo Park, California, **1978**

60 (a) Shrafy, S.; Muszkat, K. A. *J. Am. Chem. Soc.* **1971**, *93*, 4119. (b) Gegion, D.; Muszkat, K. A.; Fischer, E. *J. Am. Chem. Soc.* **1968**, *90*, 3097. (c) Saltiel, J.; Zafirion, O. C.; Megarity, E. D.; Lamola, A. A. *J. Am. Chem. Soc.* **1968**, *90*, 4759. (d) De Boer, C. D.; Schlessinger, R. H. *J. Am. Chem. Soc.*, **1968**, *90*, 803.

61 (a) Tabushi, I; Yuan, L. C. *J. Am. Chem. Soc.* **1981**, *103*, 3574. Syamala, M. S.; Devanathan, S.; Ramamurthy, V. *J. Photochem.* **1982**, *34*(2), 219. (b) Duveneck, L. G.; Sitzmann, E. V.; Eisenthal, K. B.; Turro, N. J. *J. Phys. Chem.* **1989**, *93*(20), 7166.

62 The plot of relative fluorescence intensity *vs* saccharide concentration could not be analised precisely by a simple Benesi-Hilderbrand type equation assuming the formation of a 1:1 complex.

63 A solution containing cholesteryl nanoate (1.2×10^{-5} mol), cholesteryl chloride (0.8×10^{-5} mol) and the 2:1 boronic acid saccharide complex (5.2×10^{-7} mol) in chloroform was prepared. An aliquot (200 mL) was spread on a quartz plate and mixed with minute glass beads having a uniform diameter (10±0.2mM). The sample was dried and then sandwitched between another quartz plate. The thickness of the sample prepared is then regulated by the glass beads. The wavelength of maximum reflection (λ_R = nP, where n is the mean index of reflection and P is the helical pitch of the cholesteric mesophase) was measured spectrophotometrically at 27°C. For details of the measurement method see: Shannon, P. J. *Macromolecules* **1984**, *17*, 1873.

64 Energy minimizations of the **1**/saccharide complexes was conducted using a semiempirical molecular orbital calculation method with full-geometry optimization (MOPAC ver. 6.0, AM1 Hamiltonian).[65] The imput structures for the complexes were established using the molecular modeling system (MOL-GRAPH ver3.0, Daikin Ind. Ltd.) These calculations were preformed on the engineering workstation system (SUN 4/2 and IRIS 4D/35G). The illustrations in Figure 2 were made by the ORTEPC[66] for the optimized structures.

65 MOPAC ver. 6.0, J. J. P. Stewart, QCPE #455, JCPE P049.

66 ORTEPC Rev. 1.04, C. K. Johnson, Y. Kai, T. Sei, and J. Toyoda, JCPE P039.